A polynomial expansion approach for response analysis of periodical composite structural-acoustic problems with multi-scale mixed aleatory and epistemic uncertainties

Ning Chen[1,*], Yingbin Hu[1], Dejie Yu[1], Jian Liu[1], Michael Beer[2,3,4]

[1]State Key Laboratory of Advanced Design and Manufacturing for Vehicle Body, Hunan University, Changsha, Hunan, 410082, People's Republic of China

[2] Institute for Risk and Reliability, Leibniz University Hannover, Callinstr. 34, 30167 Hannover, Germany

[3] Institute for Risk & Uncertainty, School of Engineering, University of Liverpool, Brodie Tower, Brownlow Street, Liverpool L69 3GQ, United Kingdom

[4] School of Civil Engineering & International Joint Research Center for Engineering Reliability and Stochastic Mechanics (ERSM), Tongji University, China

Abstract: The response analysis of periodical composite structural-acoustic problem with multi-scale mixed aleatory and epistemic uncertainties is investigated based on homogenization method in this paper. The aleatory uncertainties are presented by bounded random variables, whereas the epistemic uncertainties are

* Corresponding author. Tel.: +86 731 88821915; fax: +86 731 88823946.
E–mail address: chenning@hnu.edu.cn (Ning Chen)

presented by interval variables and evidence variables. When dealing with the combination of bounded random variables, interval variables and evidence variables, enormous computation is needed to estimate the output probability bounds of the sound pressure response of the periodical composite structural-acoustic system. To reduce the involved computational cost but without losing accuracy, by transforming all of the bounded random variables and interval variables into evidence variables appropriately, an evidence-theory-based polynomial expansion method (EPEM) is developed, in which the Gegenbauer series expansion is employed to approximate the variation range of the response with respect to evidence variables. By using EPEM, the probability bounds of the response can be obtained efficiently. A numerical example is used to validate the proposed method and two engineering examples are given to demonstrate its efficiency.

Key Words: Periodical composite structural-acoustic system; Homogenization method; Gegenbauer series expansion; Multi-scale uncertainty; Aleatory uncertainty; Epistemic uncertainty;

1. Introduction

To meet the needs of sustainable development, there is significant increase in the demand for lighter and more fuel-efficient materials. Composite materials can satisfy these demands and meet the requirements of stiffness as well. Consequently, composite materials are widely applied in engineering fields. In particular, more and more composites are used in the automotive and aerospace industries. However, thin, lightweight and flexible composite structures tend to vibrate and radiate noise into the

passenger compartment when excited, especially when the exciting frequency is close to the natural frequency of composite panels or the air cavity of the passenger compartment. Thus, it is significant and meaningful to conduct the vibro-acoustic analysis of composite structural–acoustic systems.

Traditional numerical methods for the frequency response analysis of the structural–acoustic system are based on deterministic physical, material and geometrical parameters [1]. However, these parameters are always associated with uncertainty in engineering practice due to the effect of aggressive environment, inevitable manufacturing errors and incomplete knowledge. The vibro-acoustic analysis results may be unreliable if these uncertainties involved in the structural–acoustic system are ignored. From this point of view, there has been increasing interest in the research of uncertain structural-acoustic systems in recent years. Xia *et al.* [2] developed a hybrid perturbation vertex method for the uncertain structural-acoustic problem with hybrid random and interval parameters. Chen *et al.* proposed a hybrid perturbation method (HPM) for the prediction of exterior acoustic field with interval and random variables [3]. Xu *et al.* studied the uncertainty propagation in SEA for structural–acoustic coupled systems with non-deterministic parameters [4]. Yin *et al.* proposed a Gegenbauer series expansion method (GSEM) to predict the response of the structure–acoustic system with hybrid bounded uncertainties [5]. Xia *et al.* developed a new optimization technique named as the optimization based on reliability and confidence interval design (O-RCID) for the optimization of the structural-acoustic system with interval probabilistic variables [6].

Though varieties of researches on uncertainty analysis of the structural-acoustic system have been done, all of those aforementioned researches are limited to structures consisting of isotropic material and the considered uncertainties are confined to macro-scale. As for periodical composite structural-acoustic systems, multi-scale uncertainties exist simultaneously. At the micro-scale, the uncertainty may come from the constituent material properties of the microstructure due to manufacturing errors. The source of the uncertainties at the macro-scale is from the physical parameters of the acoustic medium and the external load resulting from the environment. Both the uncertainties from the micro-scale and the uncertainties from the macro-scale can have an effect on the frequency response of the periodical composite structural-acoustic system. Thus, multi-scale uncertainties should be considered when analyzing periodical composite structural-acoustic systems. Up to now, Chen et al. have conducted the interval analysis for periodical composite structural-acoustic problem with multi-scale uncertain-but-bounded parameters based on perturbation method [7]. In this research, the interval analysis is based on first-order Taylor series and requires complex derivative process with respect to both macro- and micro-scale variables. This interval analysis method has its own drawbacks due to its intrusive way to handle the uncertainties. From overall perspective, researches on periodical composite structural-acoustic system with multi-scale uncertainties are meaningful and promising, but rarely reported.

In general, based on the sources of uncertainty, uncertainty can be divided into epistemic and aleatory categories [8]. The epistemic uncertainty is related to

incomplete or inaccurate information in any activity at the modeling process and can be reduced by gathering more knowledge or experimental data. On the other hand, the aleatory uncertainty comes from the inherent variation of the physical system or environment, which is usually modeled as random variable using probability theory. Up to now, random model is still considered as the most valuable mathematical model for dealing with the uncertainty existed in engineering practice. For random system response analysis, many numerical methods have been developed, such as the Monte Carlo method (MCM) [9-10], the stochastic perturbation method [11-14] and the random orthogonal polynomial approximation method [15- 20] and so on. Random model is inappropriate for the epistemic uncertainty, since even small deviation from the real probability density function (PDF) may lead to relatively large errors of the statistic response [21]. In comparison to the aleatory uncertainty analysis, the quantification of epistemic uncertainty could be more challenging. Many non-probabilistic uncertain methods have been proposed to quantify the epistemic uncertainty in a more effective way, such as the convex models [22], the possibility theory [23], the interval model [24] and the evidence theory [25-27]. Interval model can be used to model uncertain parameters whose lower and upper bounds are well defined but information about their probability density functions is missing [28- 36]. With more statistic information obtained, the belief and plausibility information of the variation range of the uncertain parameter could be acquired, and then the evidence theory can be applied to deal with the uncertainty. Among these non-probabilistic uncertain methods, evidence theory has a strong ability to handle the epistemic

uncertainty, based on which the uncertain parameters with limited information can be conveniently treated. However, in the uncertainty propagation under evidence theory model, we need to find the extreme value of the system response over each focal element, which will bring very expensive computation burden, especially when the total number of the focal elements is very large. Fortunately, the global surrogate models have been recently introduced for evidence-theory-based uncertainty analysis in order to reduce the computational cost [37-39]. In practical engineering, different kind of uncertainties may exist simultaneously. Therefore, it is necessary to build the hybrid uncertain model, which contains both aleatory uncertainty and epistemic uncertainty. The most common used one is the hybrid interval and random model [40], which has been extensively applied in many engineering fields. With more information known about the uncertain parameters of epistemic uncertainty, the hybrid uncertain model of random variables and evidence variables can be employed. Furthermore, sometimes the complex system may have interval variables, random variables and evidence variables involved simultaneously. Under this circumstance, huge computational cost is needed to estimate the output probability bounds of the system response.

The aim of this paper is to propose a numerical analysis method for the periodical composite structural-acoustic system with multi-scale mixed aleatory uncertainties and epistemic uncertainties. The aleatory uncertainties are presented by bounded random variables, whereas the epistemic uncertainties are presented by interval variables and evidence variables. When dealing with the combination of

bounded random variables, interval variables and evidence variables, enormous computation is needed to estimate the output probability bounds, especially for the periodical composite structural-acoustic system, which is a complex system and also associated with multi-scale uncertainties. Evidence theory is based on the constituted focal elements and their corresponding basic probability assignments. Under different cases, the evidence theory [37] can provide equivalent formulations to classical probability theory, possibility theory and convex models. In addition, interval model can be regarded as a special case of evidence theory model. Therefore, in this paper, to reduce the involved computational cost but without losing accuracy, all of the bounded random variables and interval variables are transformed into evidence variables appropriately. And on this basis, an Evidence-theory-based polynomial expansion method (EPEM) is developed to analysis the periodical composite structural-acoustic system with multi-scale mixed aleatory and epistemic uncertainties. The Gegenbauer series expansion method with high retained order can deal with large uncertain-but-bounded parameters, which makes it has a good application prospect in practical engineering [5]. Furthermore, the parametric Gegenbauer series polynomial holds a large number of polynomials as special cases, such as the Legendre polynomial and Chebyshev polynomial. The Gegenbauer series polynomial permits a much wider choice of polynomial bases to control the error of approximation than the traditional orthogonal polynomial approximation method. Thus, the Gegenbauer series expansion is employed to approximate the variation range of the response with respect to evidence variables in EPEM. By using EPEM, the probability bounds of the

response can be obtained efficiently.

2. The homogenization-based finite element method (HFEM) for the periodical composite structural–acoustic system

In this paper, the case we examine is a plate constructed with periodic microstructures, which is coupled with an acoustic cavity. Both the plate and the acoustic medium satisfy the linear constitutive equations and it is assumed that the acoustic medium is inviscid and incompressible. The fluid just exerts normal loads on the structure and only the normal displacement of the structure is coupled with the fluid on the interface between the structure and the fluid. The HFEM can be divided into two steps. First, obtaining equivalent material properties of the microstructure at macro-scale by conducting the homogenization analysis. Then, using the macro equivalent material properties to conduct the coupled FEM/FEM analysis of the periodical composite structural–acoustic system.

2.1. Homogenization analysis of the microstructure

In the structural–acoustic system, the macro plate is considered to consist of a kind of composite material with a periodical microstructure. Within the macroscopic domain, the microstructure is assumed to have the same configuration and uniform distribution. The micro unit cell is assumed to be composed of two different solid isotropic materials and be identical from point to point at the macro-level. Thus, the equivalent macro constitutive matrix $\mathbf{D}^{\mathrm{H}}$ of the periodical microstructure can be calculated through the homogenization method [41]

$$\mathbf{D}^{\mathrm{H}} = \frac{1}{|\Omega|}\int_{\Omega} \mathbf{D}_e \left(\mathbf{I}\text{-}\mathbf{b}\boldsymbol{\chi}\right) d\Omega \tag{1}$$

Where Ω is the domain of the micro unite cell and |Ω| represents its area; $\mathbf{D}_e$ stands for the constitutive matrix of the *e*th element in the micro unite cell; the symbol **I** is a unit matrix; the symbol **b** is the strain matrix at the micro scale; $\boldsymbol{\chi}$ represents the characteristic displacement of the microstructure. $\boldsymbol{\chi}$ satisfies the auxiliary equation which is expressed as

$$\mathbf{k}\boldsymbol{\chi} = \mathbf{f} \tag{2}$$

here, the stiffness matrix **k** and the force vector **f** of the micro unite cell at the micro-scale can be expressed as

$$\mathbf{k} = \int_{\Omega} \mathbf{b}^T \mathbf{D}_e \mathbf{b} d\Omega \tag{3}$$

$$\mathbf{f} = \int_{\Omega} \mathbf{b}^T \mathbf{D}_e d\Omega \tag{4}$$

in which the constitutive matrix $\mathbf{D}_e$ can be interpolated using the solid isotropic material with penalization (SIMP) model [42] , that is

$$\mathbf{D}_e = x_e^q \mathbf{D}^1 + \left(1 - x_e^q\right)\mathbf{D}^2 \tag{5}$$

where $\mathbf{D}^1$ and $\mathbf{D}^2$ stand for the constitutive matrices of the two given solid isotropic base material 1 and 2, respectively; x_e is the relative volumetric density, which describes the layout of the micro structure. The symbol q is the exponent of penalization, which usually is set as 3.

The average mass density η^{H} of the micro unit cell can be calculated straightforwardly as

$$\eta^{\mathrm{H}} = \frac{1}{|\Omega|}\int_{\Omega} \eta_e d\Omega \tag{6}$$

Here, η_e is the mass density of the *e*th element in the micro unit cell and can also be interpolated by the SIMP model with the exponent of penalization equals to 1,

which can be expressed as

$$\eta_e = x_e \eta^1 + (1 - x_e)\eta^2 \tag{7}$$

where η^1 and η^2 stand for the mass density of the two given solid isotropic base material 1 and 2, respectively.

2.2. FEM model for the periodical composite structural–acoustic system

In this Section, the standard coupled FEM/FEM analysis is conducted on the periodical composite structural–acoustic system [1]. Taking the structural damping into consideration, the dynamic equilibrium equation of the periodical composite structural-acoustic system under the time harmonic external excitation can be expressed as

$$\begin{bmatrix} \mathbf{K}_s + i\omega\mathbf{C}_s - \omega^2\mathbf{M}_s & -\mathbf{H} \\ \rho_f \omega^2 \mathbf{H}^{\mathrm{T}} & \mathbf{K}_f - \omega^2\mathbf{M}_f \end{bmatrix} \begin{Bmatrix} \mathbf{u}_s \\ \mathbf{p} \end{Bmatrix} = \begin{Bmatrix} \mathbf{F}_s \\ \mathbf{F}_f \end{Bmatrix} \tag{8}$$

where ω is the angular frequency of external excitation; ρ_f is the density of the acoustic fluid; $\mathbf{K}_s$ and $\mathbf{M}_s$ stand for the periodical composite structural stiffness matrix and mass matrix; $\mathbf{C}_s$ is the structural damping matrix, $\mathbf{K}_f$ and $\mathbf{M}_f$ stand for the acoustic stiffness matrix and mass matrix; $\mathbf{H}$ is the spatial coupled matrix; $\mathbf{u}_s$ and $\mathbf{p}$ are the displacement vector of periodical composite structure and the sound pressure vector in the acoustic domain; $\mathbf{F}_s$ and $\mathbf{F}_f$ are the generalized force vectors related to the periodical composite structure and to the internal acoustic cavity. The detailed derivation of Equation (8) is provided in reference [43].

The periodical composite structural stiffness matrix $\mathbf{K}_s$ and mass matrix $\mathbf{M}_s$, can be expressed as

$$\mathbf{K}_s = \sum_{j=1}^{N_{cell}} \left(\int_{\Omega_j} \mathbf{B}^{\mathrm{T}} \mathbf{D}^{\mathrm{H}} \mathbf{B} \mathrm{d}\Omega \right) \tag{9}$$

$$\mathbf{M}_s = \sum_{j=1}^{N_{cell}} \int_{\Omega_j} \eta^{\mathrm{H}} \mathbf{N}_s^{\mathrm{T}} \mathbf{N}_s \mathrm{d}\Omega \tag{10}$$

where **B** is the strain matrix at the macroscale; $\mathbf{N}_s$ is the Lagrange shape function of the isoparametric quadrilateral element; the summation represents an assembly process of the system matrices and vectors; N_{cell} is the total number of elements in the structural domain; Ω_j is the jth element in the structural domain.

The Rayleigh damping model is employed for the attached damping layer. $\mathbf{C}_s$ can be written as

$$\mathbf{C}_s = \alpha \mathbf{M}_s + \beta \mathbf{K}_s \tag{11}$$

where α and β are damping coefficients of the damping material.

The acoustic mass matrix $\mathbf{M}_f$ and stiffness matrix $\mathbf{K}_f$ can be expressed as

$$\mathbf{M}_f = \sum_{e=1}^{n_{cell}} \frac{1}{c^2} \int_{\Omega_e} \mathbf{N}_f^{\mathrm{T}} \mathbf{N}_f \mathrm{d}\Omega \tag{12}$$

$$\mathbf{K}_f = \sum_{e=1}^{n_{cell}} \int_{\Omega_e} (\nabla \mathbf{N}_f)^{\mathrm{T}} \cdot (\nabla \mathbf{N}_f) \mathrm{d}\Omega \tag{13}$$

in which n_{cell} is the total number of elements in the acoustic domain; Ω_e is the eth element in the acoustic domain; $\mathbf{N}_f$ is the Lagrange shape function of the isoparametric hexahedral element; c is the speed of the sound.

In order to simplify the process of analyzing the dynamic equilibrium equation of the periodical composite structural–acoustic system, we rewrite Eq. (8) as the following form

$$\mathbf{ZU} = \mathbf{F} \tag{14}$$

where **Z** is the periodical composite structural-acoustic dynamic stiffness matrix; **U** is the frequency response vector; **F** is the external excitation vector. They can be expressed as

$$\mathbf{Z}=\begin{bmatrix}\mathbf{K}_s+i\omega\mathbf{C}_s-\omega^2\mathbf{M}_s & -\mathbf{H}\\ \rho_f\omega^2\mathbf{H}^{\mathrm{T}} & \mathbf{K}_f-\omega^2\mathbf{M}_f\end{bmatrix},\ \mathbf{U}=\begin{Bmatrix}\mathbf{u}_s & \mathbf{p}\end{Bmatrix}^{\mathrm{T}},\ \mathbf{F}=\begin{Bmatrix}\mathbf{F}_b & \mathbf{F}_q\end{Bmatrix}^{\mathrm{T}} \quad (15)$$

3.Three uncertain models

In practical engineering problems, uncertainties in material properties, geometric dimensions, environmental parameters and external loads are unavoidable. The uncertain parameters are always bounded because of the limitations in design tolerance. For the system with several uncertain parameters, we denote these parameters with a bounded vector $\mathbf{x}=[x_1,x_2,...,x_L]$, which satisfies $\underline{\mathbf{x}} \le \mathbf{x} \le \overline{\mathbf{x}}$. The symbols $\underline{\mathbf{x}}$ and $\overline{\mathbf{x}}$ respectively denote the lower bound and the upper bound vectors.

3.1. Interval model

Because of the limited information, the uncertain parameters only their lower and upper bounds can be obtained are modeled as the interval variables. The *L*-dimensional interval vector **x** can be expressed as

$$\mathbf{x}=\mathbf{x}^I=[\underline{\mathbf{x}},\overline{\mathbf{x}}]=[x_1^I,x_2^I,...,x_L^I]\ ,\ \ x_s^I=[\underline{x}_s,\overline{x}_s],\ s=1,2,\ldots,L. \quad (16)$$

Where $\underline{\mathbf{x}}$ and $\overline{\mathbf{x}}$ are the lower and upper bounds of the interval vector $\mathbf{x}^I$; $\underline{x}_s$ and $\overline{x}_s$ are the lower and upper bounds of the interval parameter x_s^I.

3.2. Evidence theory

With the statistic information increasing but not adequate to define the PDF precisely, the evidence theory can be employed to handle the uncertain parameters.

Evidence theory, also called as the Dempster–Shafer theory, was firstly proposed by Dempster and further developed by Shafer. The main concept of evidence theory is that our knowledge on a given problem can be inherently imprecise. With the belief and plausibility of the interval obtained, uncertain parameters can be modeled as evidence variables. The basic concept of evidence theory is given in Appendix A.

The L-dimensional evidence vector $\mathbf{x}$ can be expressed as

$$\mathbf{x} = \mathbf{x}^E = [x_1^E, x_2^E, ..., x_L^E]. \tag{17}$$

3.3. Bounded random model

When the information is enough to construct the PDF precisely in the variation range [44], the bounded random model is a valuable mathematical model to treat the uncertain parameters in engineering practices. When the PDF of variable x_i is well defined, x_i can be modeled by a bounded random variable x_i^R and the bounded random variable x_i^R satisfies

$$\begin{cases} p(x_i^R) > 0, & x_i^R \in [\underline{x}_i, \overline{x}_i] \\ p(x_i^R) = 0, & \text{else} \end{cases} \tag{18}$$

where $p(x_i^R)$ is the PDF of x_i^R. It is noted here that the bounded random variables are a special case of random variables because its variation range is finite.

The L-dimensional uncertain-but-bounded random vector $\mathbf{x}$ can be expressed as

$$\mathbf{x} = \mathbf{x}^R = [x_1^R, x_2^R, ..., x_L^R] \tag{19}$$

3.4. Definition of the hybrid model

For a complex engineering system, different type of uncertain parameters may exist simultaneously. In this paper, the considered case includes bounded random variables, evidence variables and interval variables. The bounded random model is

used to handle the parameters whose PDFs are defined unambiguously due to sufficient information. However, we can't get the precise PDF of uncertain parameter in most situations because of insufficient information or knowledge. Then, using a confidence interval instead of a deterministic value to depict the total degree of probability in a proposition seems more reasonable. In general, evidence theory uses the belief and plausibility to quantify the lower and upper bounds of the precise probability. Besides, the interval model is used to treat the uncertain parameters whose information about the probability assignment is missing but the upper and lower bounds are available. The hybrid model can be expressed as

$$\mathbf{x} = [\mathbf{x}^R, \mathbf{x}^E, \mathbf{x}^I] = [x_1^R, x_2^R, ..., x_{L_1}^R, x_{L_1+1}^E, ..., x_{L_2}^E, x_{L_2+1}^I, ..., x_L^I]. \quad (20)$$

Where, x^R denotes bounded random variable, x^E denotes evidence variable, and x^I denotes bounded interval variable.

3.5. Transformation of variables in the hybrid model

The differences among bounded random variables, evidence variables and interval variables are just the amount of available information. The required information of bounded random variables is to construct the PDFs, whereas the required information of evidence variable is to depict the degree of probability in every focal element. The required information of interval variable is the least. Only the information about lower and upper bounds are needed. As is mentioned above, the evidence variable is a versatile tool, which can be used to deal with bounded random variable and interval variable. In this paper, we use evidence variable to substitute the bounded random variable and interval variable. Certainly, the interval variable can be

treated as an evidence variable who has just one focal element. For a bounded random variable x_i^R, the variation interval of x_i^R can be divided into many small intervals, which can be treated as focal elements of evidence variable, whose BPA can be obtained by integrating the PDF of bounded random variable in the corresponding interval. The bounded random variable is equal to an evidence variable when the transformed focal elements of bounded random variable increase to infinity, which can be seen from Fig. 1. In Fig. 1, the x represents a bounded random variable or an evidence variable. The horizontal axis represents the value of x and vertical axis represents the probability density of x. The area of the rectangle represents the BPA of the evidence variable. For a system, when the involved bounded random variable is transformed into evidence variable, the CBF and CPF of the system response will gradually be converged with the number of focal elements increasing. By comparing the CBF and CPF of system response with different number of focal elements, an appropriate number of focal elements with sufficient accuracy can be acquired. In conclusion, by choosing the focal element number properly, the bounded random variable and interval variable can be transformed into evidence variable. That is to say, the hybrid model can be transformed into pure evidence-theory model.

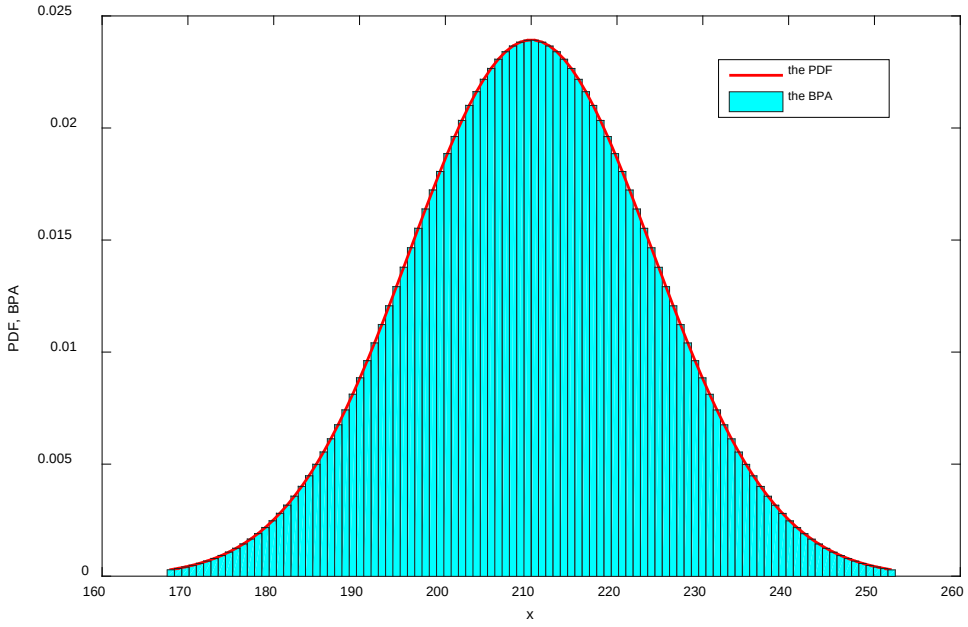

Fig. 1 The transformation from a random variable to an evidence variable

4. EPEM for the analysis of periodical composite structural-acoustic system with multi-scale evidence variables

For the periodical composite structural-acoustic system with multi-scale mixed aleatory and epistemic uncertainties, to reduce the involved computational cost and assure the accuracy, all of the bounded random variables and interval variables are transformed into evidence variables appropriately. An Evidence-theory-based polynomial expansion method (EPEM) is presented in this section to predict the response of periodical composite structural-acoustic system with multi-scale evidence variables.

4.1. Transformation of evidence variables

The focal elements of the evidence variable in practical engineering are arbitrary interval. However, the Gegenbauer series expansion is defined on [-1,1]. In order to apply the Gegenbauer series expansion here, we can transform evidence variable x_i

into the linear function of the unitary evidence variable $\xi_i \in [-1,1]$ as follows

$$\mathbf{x} = \mathbf{X}(\boldsymbol{\xi}),\ \mathbf{x} = [x_1, x_2, ..., x_L],\ \boldsymbol{\xi} = [\xi_1, \xi_2, ..., \xi_L] \tag{21}$$

$$x_i = X_i(\xi_i) = a_{i,0} + a_{i,1}\xi_i,\ \ i = 1, 2, ..., L \tag{22}$$

where

$$a_{i,0} = \frac{\overline{x}_i + \underline{x}_i}{2},\ a_{i,1} = \frac{\overline{x}_i - \underline{x}_i}{2}. \tag{23}$$

Meanwhile, an arbitrary focal element $\tilde{A}_i$ of x_i will be transformed into $\tilde{B}_i$, which satisfies the following conditions

$$\begin{cases} \tilde{A}_i = a_{i,0} + a_{i,1}\tilde{B}_i \\ m(\tilde{A}_i) = m(\tilde{B}_i) \end{cases}. \tag{24}$$

4.2. Gegenbauer series expansion for the response of the periodical composite structural-acoustic system with multi-scale evidence variables

There are numerous orthogonal polynomial approximation methods can be applied on the analysis of periodical composite structural-acoustic system with multi-scale evidence variables [37, 45]. Gegenbauer series expansion method is just one of these polynomial approximation methods that can approximate the response of the system with enough accuracy. It has a good efficiency and can achieve high accuracy with the number of retained order increases. The fundamental idea of approximation theory of Gegenbauer series expansion is given in Appendix B.

The first step is to expand the response **U** at the bounds of evidence variable vector **x**. Theoretically, the polynomial parameter λ of Gegenbauer series expansion for interval can take any value satisfying $\lambda > 0$. Nevertheless, different value of λ can result in different accuracy of Gegenbauer series expansion for interval problems. It is found that the accuracy of Gegenbauer series expansion will increase with the

decrease of λ [5]. Generally, the λ in practical interval problems will be taken a small value, and marked as λ^0. Thus, the λ for evidence variables are also taken a small value in this paper.

Based on the transformation of evidence variables in Eqs. (21-23) and the theory of Gegenbauer series expansion, the response of the periodical composite structural-acoustic system with multi-scale evidence variables can be approximated as

$$\mathbf{U}=\mathbf{U}(\mathbf{x})=\mathbf{U}\left(\mathbf{X}(\boldsymbol{\xi})\right)=\sum_{i_1=0}^{N_1}\cdots\sum_{i_L}^{N_L}\mathbf{f}_{i_1,\ldots,i_L}G_{i_1,\ldots,i_L}^{\lambda^0,\ldots,\lambda^0}(\boldsymbol{\xi}) \tag{25}$$

where

$$\mathbf{f}_{i_1,\ldots,i_L}\approx\frac{1}{h_1^{\lambda^0}\times\cdots\times h_L^{\lambda^0}}\sum_{j_1=1}^{M_1}\cdots\sum_{j_L=1}^{M_L}\mathbf{U}\left(\mathbf{X}^I(\hat{\xi}_{j_1}^{\lambda^0},\ldots,\hat{\xi}_{j_L}^{\lambda^0})\right)G_{i_1,\ldots,i_L}^{\lambda^0,\ldots,\lambda^0}(\hat{\xi}_{j_1}^{\lambda^0},\ldots,\hat{\xi}_{j_L}^{\lambda^0})A_{i_1,\ldots,i_L}^{\lambda^0,\ldots,\lambda^0}. \tag{26}$$

Then, for the system with *L* evidence variables**,** the joint FD for evidence variables vector $\mathbf{x}=[x_1,x_2,\ldots,x_L]$ can be defined using the Cartesian product and denoted by **S** as follows.

$$\begin{aligned}\mathbf{S}&=x_1\times x_2\times\cdots\times x_L\\&=\{\mathbf{s}_k=[u_1,u_2,\ldots,u_L],u_j\in x_j,\ j=1,2,\ldots,L,k=1,2,\ldots,n_s\}\end{aligned}. \tag{27}$$

Where, u_j denotes the focal element of x_j, $\mathbf{s}_k$ denotes the focal element of the joint FD, n_s is the total number of $\mathbf{s}_k$. Supposing the number of focal elements for the *j*th evidence variable is l_j (j = 1, 2, . . . , L), then the total number of $\mathbf{s}_k$ is $n_s = l_1 \times l_2 \times \cdots \times l_L$.

Referring to Eq. (24), the Cartesian product **T** of the transformed evidence variables vector can be depicted as

$$\begin{aligned}\mathbf{T}&=\xi_1\times\xi_2\times\cdots\times\xi_L\\&=\{\mathbf{t}_k=[\psi_1,\psi_2,\ldots,\psi_L],\psi_j\in\xi_j,\ j=1,2,\ldots,L,k=1,2,\ldots,n_s\}\end{aligned} \tag{28}$$

where, ψ_j denotes the focal element of ξ_j, $\mathbf{t}_k$ denotes the focal element of the joint FD.

Substituting $\mathbf{t}_k$ into the expansion function as shown in Eq. (25), one gets the approximated expression of the corresponding response $\mathbf{U}_k(\mathbf{t}_k)$,

$$\mathbf{U}_k(\mathbf{t}_k) = \sum_{i_1=0}^{N_1} \cdots \sum_{i_L}^{N_L} \mathbf{f}_{i_1,\ldots,i_L} G_{i_1,\ldots,i_L}^{\lambda^0,\ldots,\lambda^0}(\mathbf{t}_k). \tag{29}$$

The lower and upper bounds of the response $\mathbf{U}_k$ can be calculated by the Monte Carlo method. Assuming the sampling points for the focal element of the joint FD $\mathbf{t}_k$ is $\tilde{\mathbf{t}}_{ki}$ $(i = 1, 2, ..., n_p)$. Here, n_p denotes the number of the sampling points. By substituting these sampling points into the Eq. (29), we get a series of corresponding responses, which are denoted as a vector $\mathbf{U}_k(\tilde{\mathbf{t}}_{ki})$. Then, the lower and upper bounds of the response vector $\mathbf{U}_k$ can be obtained as

$$[\underline{\mathbf{U}}_k, \overline{\mathbf{U}}_k] = \left[\min\left\{ \mathbf{U}_k(\tilde{\mathbf{t}}_{ki}) \right\}, \max\left\{ \mathbf{U}_k(\tilde{\mathbf{t}}_{ki}) \right\} \right]. \tag{30}$$

The BPA of the response $\mathbf{U}_k$ can be calculated through the following equations.

$$m(\mathbf{U}_k) = m(\mathbf{t}_k) = \begin{cases} \prod_{j=0}^{L} m(\psi_j) \\ 0 \qquad otherwise \end{cases}. \tag{31}$$

Where, $m(\mathbf{t}_k)$ denotes the BPA of the response $\mathbf{t}_k$ and $m(\psi_j)$ denotes the BPA of the focal element in ξ_j. $m(\psi_j)$ can be calculated through the Eq. (24) and expressed as

$$m(\psi_j) = m(u_j). \tag{32}$$

Here, $m(u_j)$ is the BPA of focal element in evidence variable x_j.

The CBF and CPF of **U** can be calculated as follow: (1) sorting out the $\underline{\mathbf{U}}_k$ and $\overline{\mathbf{U}}_k$ from the smallest to the largest and getting a response vector, which is noted as

$\mathbf{U}_j$ ($j=1,2,...,2n_s$); (2) conducting the follow operation

$$\mathrm{CBF}(\mathbf{U}=\mathbf{U}_j)=\sum_{\underline{\mathbf{U}}_k\le\mathbf{U}_j} m(\mathbf{t}_k) \tag{33}$$

$$\mathrm{CPF}(\mathbf{U}=\mathbf{U}_j)=\sum_{\underline{\mathbf{U}}_k\le\mathbf{U}_j} m(\mathbf{t}_k) \tag{34}$$

The fundamental idea of CBF and CPF is introduced in Appendix A.1.

4.3. The procedure of the proposed EPEM for the periodical composite structural-acoustic system with multi-scale evidence variables

For the periodical composite structural-acoustic system with multi-scale mixed aleatory and epistemic uncertainties, an evidence-theory-based method is proposed in this paper. By transforming all the bounded random variables and interval variables into evidence variables and then applying orthogonal polynomial approximation method on this periodical composite structural-acoustic system, the involved computational cost can be greatly reduced. The procedure of the proposed EPEM can be summarized as follows

(1) Discretize the macro structural–acoustic system and microstructure design domain by a finite element mesh with given boundary and loading condition;

(2) Transform the bounded random variables into evidence variables with proper number of focal elements. In addition, treat the interval variables as evidence variables with one focal element;

(2) Calculate the transformation coefficient $a_{i,0}$ and $a_{i,1}$, then select a small positive value for the polynomial parameter λ with respect to each evidence variables. λ can be selected arbitrarily. $a_{i,0}$ and $a_{i,1}$ is determined through Eq. (23);

(3) Calculate the interpolation points and the weights of Gauss-Gegenbauer integration with respect to each evidence variable through Eq. (B.14);

(4) Perform the finite element analysis on the micro scale to calculate the effective elastic matrix $\mathbf{D}^{\mathrm{H}}$ and the average mass density η^{H} at the interpolation points based on the homogenization method, then calculate the responses of periodical composite structural-acoustic system at the interpolation points through Eq. (15);

(5) Calculate the expansion coefficients of Gegenbauer series through Eq. (26) for the evidence variables.

(6) Calculate the CBF and CPF of the response through Eqs. (33) and (34).

It should be noted that the Gegenbauer series expansion method is not the only method to approximate response of periodical composite structural-acoustic system. The Jacobi expansion [37], the Legendre polynomial [45] and the Chebyshev polynomial [36] can also be adopted in the proposed method.

5. Numerical examples

In this section, a numerical example and two engineering examples are presented to verify the effectiveness of the proposed method. The reference results can hardly be calculated through MCM for engineering examples because of the tremendous computational burden. For example, assume there are one bounded random variable, one evidence variable and two interval variables existed in the periodical composite structural-acoustic system. The bounded random variable is transformed into an evidence variable with 100 focal elements and the interval variables are transformed into evidence variables with one focal elements. The evidence variable is assumed to

consist of 16 focal elements. Then the joint FD of these evidence variables has 1600 focal elements. Supposing that the samples of the MCM in each focal element of joint FD are set as 10000, the computation amount of MCM can be estimated, which is 16 million times calls of deterministic calculation of the periodical composite structural-acoustic system. However, it will take several seconds to conduct one time computation through the present computing power for the frequency response of the hexahedral box and automobile passenger compartment model. Thus, the reference results for two engineering examples are not given. Nevertheless, a simple function presented in Section 5.1 is firstly used to validate the effectiveness of the proposed method.

5.1. A simple function

In this section, a simple function is defined to examine the accuracy of the proposed method. For brevity but without loss of generality, the function can be defined as

$$y = \arctan^3 x_1 + x_1^2 - 2\arctan^{1/2} x_2 - 2^{x_3} + 0.2x_4^2 + 0.5x_4 + \frac{x_2^{x_3}}{x_4} + 0.2x_1x_2x_3 \tag{35}$$

where, variables x_i (i = 1, 2, 3, 4) are dimensionless uncertain variables. x_1 and x_2 are interval variables, x_1 = 2[1-α, 1+α] and x_2 = 4[1-α, 1+α]. x_3 is a bounded random variable and x_4 is an evidence variable. x_3 and x_4 is defined as x_3 = 3[1-α, 1+α] and x_4 = 1[1-α, 1+α]. α is the uncertain level, which is set as 0.2 here. It's assumed that the evidence variable and bounded random variable are derived from the truncated normal distribution. The expectation and standard variance of x_3 and x_4

are $\mu(x_3)$=3 , $\sigma(x_3)$=1 and $\mu(x_4)$=1 , $\sigma(x_4)$=1/3 respectively. The evidence variable x_4 contains 16 focal elements, whose BPAs are given in Table 1. The retained order and polynomial parameters for each variable are set as $\lambda_{x_1}=\lambda_{x_2}=\lambda_{x_3}=\lambda_{x_4}=0.001$, $n_{x_1}=n_{x_2}=n_{x_3}=n_{x_4}=3$. Simulations of this example are carried out by MATLAB R2015a on a 2.93GHz Core(TM) 8 CPU E7500.

Table 1. The BPAs for the evidence variable x_4 with 16 focal elements.

Focal elements	BPA	Focal elements	BPA
[2.400, 2.475]	0.0030	[3.000, 3.075]	0.1462
[2.475, 2.550]	0.0079	[3.075, 3.150]	0.1272
[2.550, 2.625]	0.0182	[3.150, 3.225]	0.0963
[2.625, 2.700]	0.0364	[3.225, 3.300]	0.0635
[2.700, 2.775]	0.0635	[3.300, 3.375]	0.0364
[2.775, 2.850]	0.0963	[3.375, 3.450]	0.0182
[2.850, 2.925]	0.1272	[3.450, 3.525]	0.0079
[2.925, 3.000]	0.1462	[3.525, 3.600]	0.0030

The CBF and the CPF of y are calculated through EPEM and depicted in Fig. 2 where the bounded random variable is transformed into evidence variable with 10, 100 and 200 focal elements respectively. It can be seen from Fig. 2 that the result when the bounded random variable is transformed into evidence variable with 100 focal elements is almost the same as the result when the bounded random variable is transformed into evidence variable with 200 focal elements. Whereas, the results obviously deviate from the converged results when the transformed evidence variable

just contains 10 focal elements. This indicates that when the random variable is transformed into an evidence variable with 100 focal elements, the result is converged and can be calculated with sufficient accuracy. Thus, the bounded random variable x_3 is transformed into evidence variable with 100 focal elements.

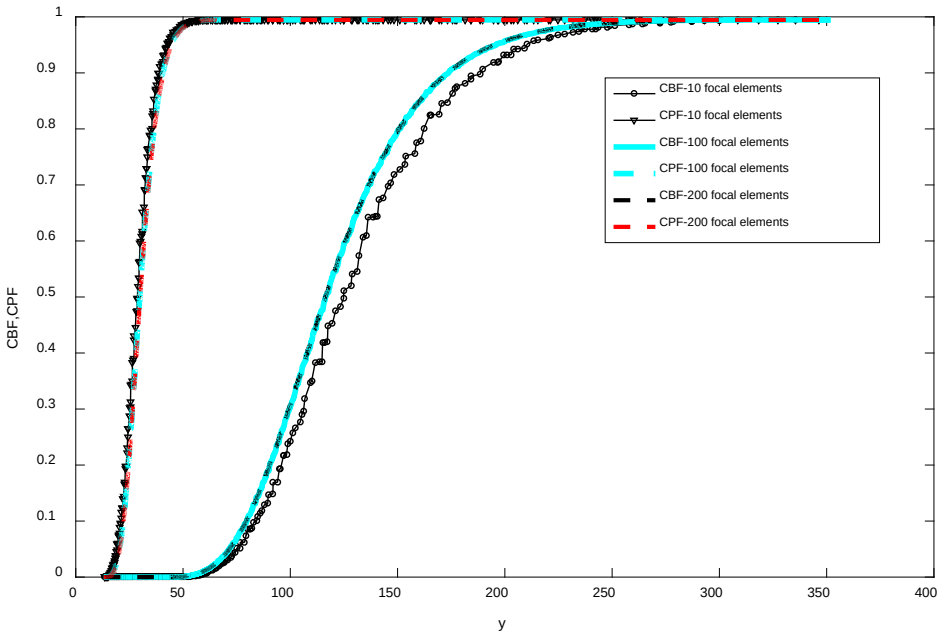

Fig. 2 The CBF and CPF of y when the bounded random variable is transformed into evidence variable with 10, 100 and 200 focal elements respectively

The CBF and CPF of the function value y calculated by using the proposed EPEM and MCM are compared in Fig. 3. Here, the results obtained by MCM are used as reference. It can be seen from Fig. 3 that the CBF and CPF computed by EPEM have a great agreement with those computed by MCM, which indicates that the proposed EPEM is feasible and of great accuracy. In the computational process of using EPEM, the simple function was called for $n = (n_{x_1} + 1) \times (n_{x_2} + 1) \times (n_{x_3} + 1) \times (n_{x_4} + 1) = 4^4 = 256$ times, while the MCM has to call the function for 16 million times. Therefore, it has been proved that the EPEM is far more efficient than the MCM but with maintaining high accuracy.

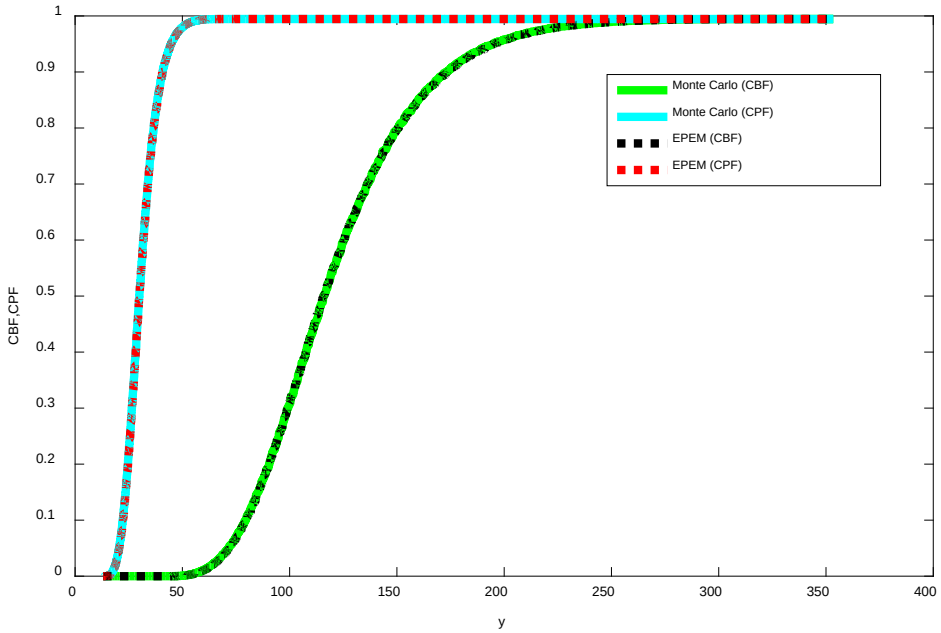

Fig. 33 The CBF and CPF of y

5.2. A hexahedral box

A cavity enclosed by a hexahedral box of dimensions 0.25m × 0.25m ×0.25m is shown in Fig. 4. The acoustic field is surrounded by five rigid walls and a clamped plate. The center of the top surface is excited by a concentrated harmonic load F=10 N. The density of the air is 1.21 kg/m^3, and the sound speed of the air 336.9 m/s. The damping coefficients are set as α=0.5 and β=0.1. The clamped plate is discretized by 64 four-node Kirchhoff plate elements and the acoustic domain is discretized by 512 eight-node hexahedral elements. The central line depicted in Fig. 4 is used to observe the sound pressure response in the acoustic field. The x-coordinate of the leftmost point at the central line is 0 mm and the x-coordinate of the rightmost point at the central line is 250 mm.

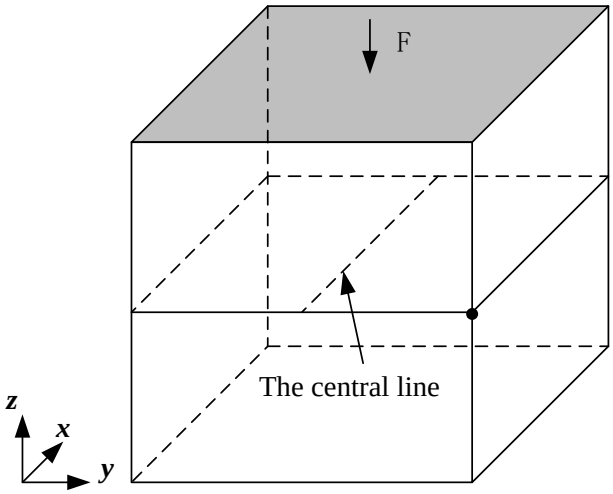

Fig. 4 A hexahedral box

The macro clamped plate is considered to be composed of a periodic uniform material. The homogenization analysis can be performed to calculate the equivalent macro material properties. A unit Representative Volume Element (RVE) of the unidirectional fiber reinforced composite is depicted in Fig. 5. For simplicity, it is assumed that the unit cells at the micro scale are square and with a dimensionless length of 1 × 1. The radius of the fiber in the center of the matrix is 0.2. The finite element model of the RVE is composed of 361 nodes and 340 elements. The microstructure unit cell consists of two prescribed materials, namely, the strong material (Red color) and the soft material (Green color). The Young's modulus, mass density and the Poisson's ratio of strong material are E_1 =210 GPa, ρ_1 =7800 kg/m^3 and v_1=0.3, respectively. The soft material in the unit cell has $E_2 = E_1 / 10$, $\rho_2 = \rho_1 / 10$, and $v_2 = 0.3$.

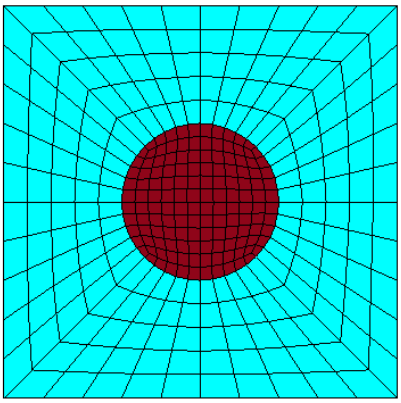

Fig. 5 RVE of a unidirectional fiber reinforced composite

At the micro-scale, considering the unpredictability of the material properties, the Young's modulus of the fiber and the matrix are assumed to be interval variables, which are E_1 = 210[1-α, 1+α] GPa and E_2 = 21[1-α, 1+α] GPa, respectively. α is the uncertain level. At the macro-scale, the thickness of the plate and the sound speed of the air are respectively assumed to be evidence variable and bounded random variable, whose variation ranges are t = 1[1-α, 1+α] mm and c = 336.9[1-α, 1+α] m/s, respectively. The expectation and standard variance of the bounded random variable are $\mu(c)$=336.9 m/s and $\sigma(c)$=112.3 m/s, respectively. In this numerical example, the bounded random variable c who follows the normal distribution is transformed into evidence variable with 100 focal elements, which is depicted in Fig. 6. The evidence variable t who contains 16 focal elements is derived from a truncated normal distribution random variable whose expectation and standard variance are $\mu(t)$=1 mm, $\sigma(t)=1/3$ mm. The BPAs of the evidence variable t are given in Table 2. The retained order and polynomial parameters for each uncertain variable are set as $\lambda_{E_1}=\lambda_{E_2}=\lambda_c=\lambda_t=0.001$, $n_{E_1}=n_{E_2}=n_c=n_t=3$. Due to the excessive computation burden of the Monte Carlo simulation approach, the reference results are not given.

Simulations of this hexahedral box are carried out by MATLAB R2015a on a 2.93GHz Core(TM) 8 CPU E7500.

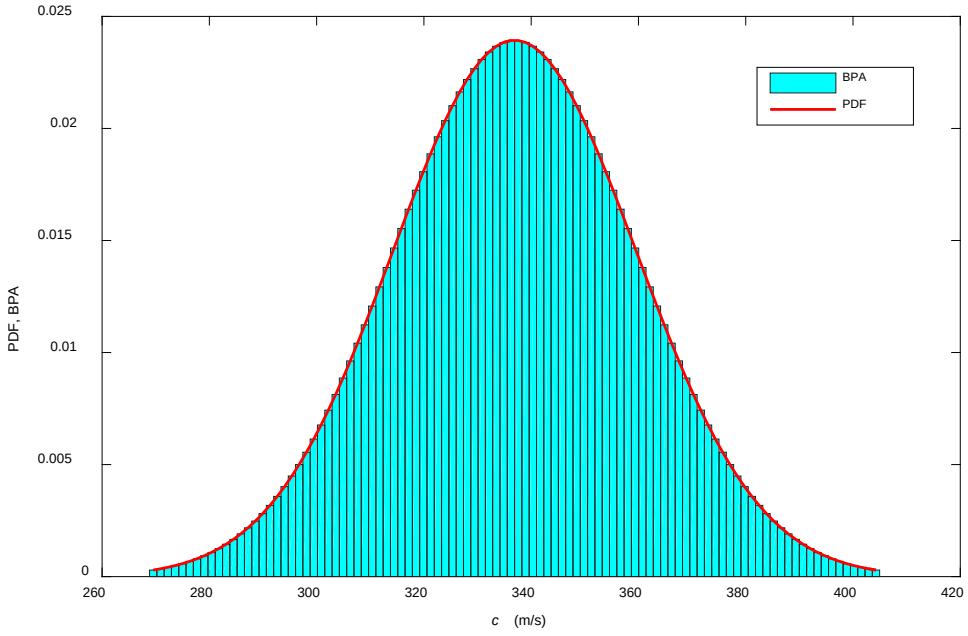

Fig. 6 The transformation of the bounded random variable *c*.

Table 2. The BPAs for the evidence variable *t* with 16 focal elements.

Focal elements (mm)	BPA	Focal elements (mm)	BPA
[0.800, 0.825]	0.0030	[1.000, 1.025]	0.1462
[0.825, 0.850]	0.0079	[1.025, 1.050]	0.1272
[0.850, 0.875]	0.0182	[1.050, 1.075]	0.0963
[0.875, 0.900]	0.0364	[1.075, 1.100]	0.0635
[0.900, 0.925]	0.0635	[1.100, 1.125]	0.0364
[0.925, 0.950]	0.0963	[1.125, 1.150]	0.0182
[0.950, 0.975]	0.1272	[1.150, 1.175]	0.0079
[0.975, 1.000]	0.1462	[1.175, 1.200]	0.0030

To prove the result obtained by the proposed EPEM is correct, we computed a

series of random CBF and CPF lines of the sound pressure amplitude at the point x = 0 mm when f = 50 Hz and α = 0.2, as shown in Fig. 7. Besides, Fig. 7 shows the CBF and CPF of the sound pressure amplitude at the point x = 0 mm calculated by EPEM. The CBF and CPF yielded by EPEM are marked as EPEM (CBF), EPEM (CPF). The series of random CBF and CPF lines of the sound pressure amplitude are obtained through the following process. Firstly, we randomly sample two points in the variation range of every focal element with respect to each uncertain variable. $\tilde{\mathrm{E}}_{1i}$ and $\tilde{\mathrm{E}}_{2i}$ are assumed to be the random points of E_1 and E_2, respectively. $\tilde{c}_{ni}$ is assumed to be the random points of the nth focal element of c and $\tilde{t}_{mi}$ are assumed to be the random points of the mth focal element of t (i =1,2. n=1, 2, 3,…,100. m=1, 2, 3,…, 16). By substituting $\tilde{\mathrm{E}}_{11}$, $\tilde{\mathrm{E}}_{21}$, $\tilde{c}_{n1}$ and $\tilde{t}_{m1}$ into the Eq. (15), we can get a series of response $\mathbf{U}_{k1}$. Similarly, $\mathbf{U}_{k2}$ can be calculated by substituting $\tilde{\mathrm{E}}_{12}$, $\tilde{\mathrm{E}}_{22}$, $\tilde{c}_{n2}$ and $\tilde{t}_{m2}$ into the Eq. (15). Denote the larger one and the smaller one of $\mathbf{U}_{k1}$ and $\mathbf{U}_{k2}$ as $\overline{\mathbf{U}}_k$ and $\underline{\mathbf{U}}_k$, respectively. Then one CBF line and one CPF line can be computed through Eqs. (31-34). Repeating for 100 times, 100 random CBF lines and 100 corresponding CPF lines can be obtained. It can be seen from Fig. 7 that these random CBF and CPF lines are all enveloped by the CBF and CPF line computed by EPEM. This indicates that the proposed EPEM can predict the output probability bounds of the sound pressure amplitude of the periodical composite structural-acoustic system with multi-scale mixed aleatory and epistemic uncertainties.

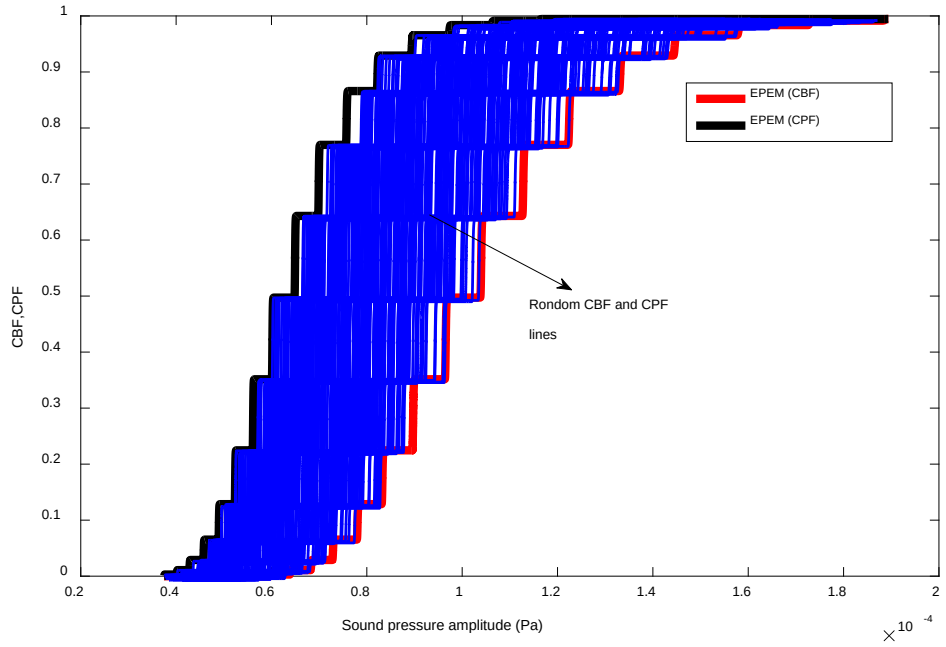

Fig. 7 The CBF and CPF of the sound pressure amplitude when f = 50 Hz and x = 0 mm

The CBF and the CPF of the sound pressure amplitude at two different points on the central line are calculated by EPEM when f = 200 Hz and α =0.2. The results are shown in Fig. 8. The considered frequency is 200 Hz. The selected point is x = 0 mm and x = 31.25 mm. It can be seen from Fig. 8 that the cumulative plausibility value is larger than the cumulative belief value. This is reasonable because the cumulative plausibility value is an optimistic estimation and the cumulative belief value is a conservative estimation. In engineering practice, the acoustic behavior is considered in structural design and optimization to achieve high level NVH performance. By comparing the result obtained by the EPEM method with the desired demand, the optimistic and conservative reliability of the structural design considering acoustic behavior can be estimated. Therefore, the EPEM for the periodical composite structural-acoustic coupled system with multi-scale mixed aleatory and epistemic uncertainties is practical.

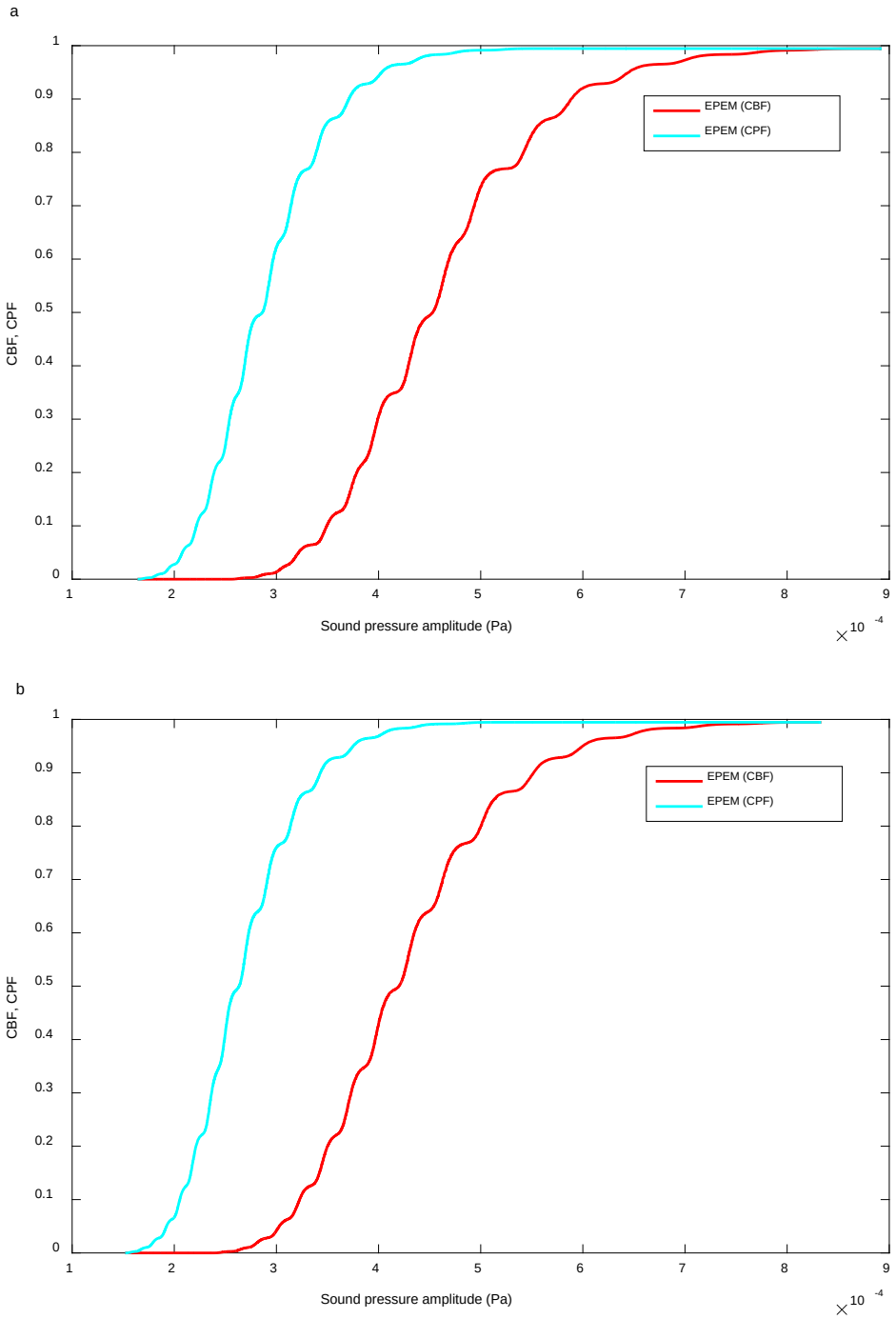

Fig. 8 The CBF and CPF of the sound pressure amplitude when f = 200 Hz: (a) x = 0 mm (b) x = 31.25 mm.

The 90% interpercentile range of sound pressure amplitude under optimistic and conservative estimation when f = 50-200 Hz and x = 0 mm is depicted in Fig. 9. Here, the 90% interpercentile ranges of the frequency response amplitude are the optimistic and conservative estimation for the frequency response amplitude when the value of

cumulative probability function is between 5% and 95%. It can be seen that the lower and upper bounds of the conservative estimation are bigger than that of the optimistic estimation. It is reasonable because usually more confronting situations are considered in the conservative estimation than those considered in the optimistic estimation.

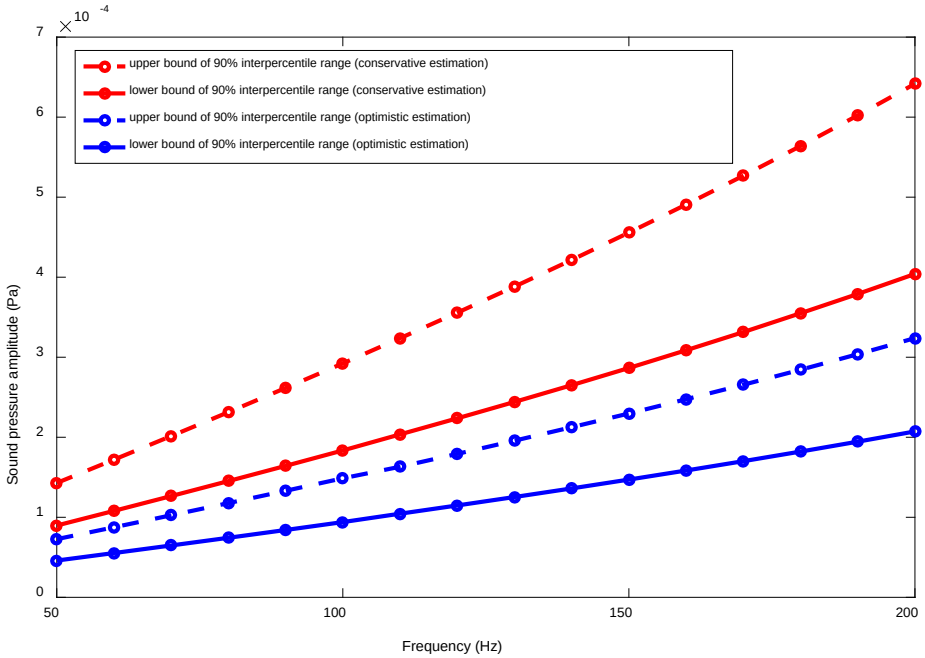

Fig. 9. The 90% interpercentile range of sound pressure amplitude under optimistic and conservative estimation for f = 50-200 Hz and x = 0 mm

5.3. An automobile passenger compartment

Fig. 10 depicts an automobile passenger compartment with flexible roof panel. The roof is excited by a unit normal harmonic point force at the center. The thickness of the roof panel is 1 mm. The four sides of the roof panel are set to be fixed. The density and the sound speed of the air are 1.21 kg/m^3 and 336.9 m/s, respectively. The node A is near the driver's left ear. The macro roof panel is assumed to be composed of a periodic uniform material. The microstructure unit cell consists of two prescribed materials. The two materials employed and the unit Representative Volume Element

of the unidirectional fiber reinforced composite are the same as those in Section 6.2. At the micro-scale, considering the unpredictability of the material properties, the Young's modulus of the fiber and the matrix are assumed to be interval variables, which are $E_1 = 210[1-\alpha, 1+\alpha]$ GPa and $E_2 = 21[1-\alpha, 1+\alpha]$ GPa, respectively. α is the uncertain level. At the macro-scale, the thickness of the plate and the sound speed of the air are respectively assumed to be evidence variable and bounded random variable, whose variation ranges are $t = 1[1-\alpha, 1+\alpha]$ mm and $c = 336.9[1-\alpha, 1+\alpha]$ m/s, respectively. The bounded random variable c is transformed into an evidence variable with 100 focal elements, as shown in Fig. 5. The evidence variable t contains 16 focal elements, whose corresponding BPAs are given in Table 2. The retained order and polynomial parameters for each variable are set as $\lambda_{E_1} = \lambda_{E_2} = \lambda_c = \lambda_t = 0.001$, $n_{E_1} = n_{E_2} = n_c = n_t = 3$. The CBF and CPF of the frequency response are calculated using the proposed EPEM. The reference results computed by MCM are not given in this example due to excessive computation burden. Simulations of this automobile passenger compartment are carried out by MATLAB R2015a on a 2.93GHz Core(TM) 8 CPU E7500.

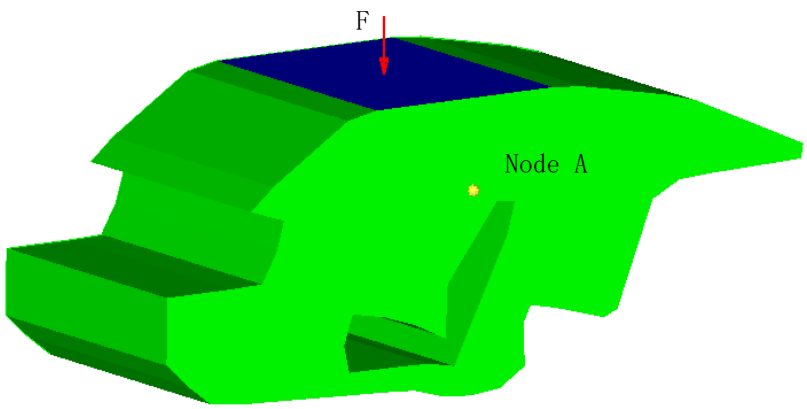

Fig. 10 An automobile passenger compartment

The CBF and CPF of the sound pressure amplitude at node A calculated by EPEM when α =0.2 are shown in Fig. 11. The considered frequency is 50 Hz. 100 pairs of random CBF and CPF lines of the sound pressure amplitude at node A are also computed to validated the effectiveness of the EPEM when α =0.2 and f=50Hz, as shown in Fig. 11. These random CBF and CPF lines of the sound pressure amplitude at node A are calculated through the same process as used in the last numerical example. It can be seen from Fig. 11 that these random CBF and CPF lines are all enveloped by the CBF and CPF line computed by EPEM, which examines the correctness of the results obtained by EPEM. This further indicates that the EPEM can be used for the analysis of periodical composite structural-acoustic coupled system with multi-scale mixed aleatory and epistemic uncertainties.

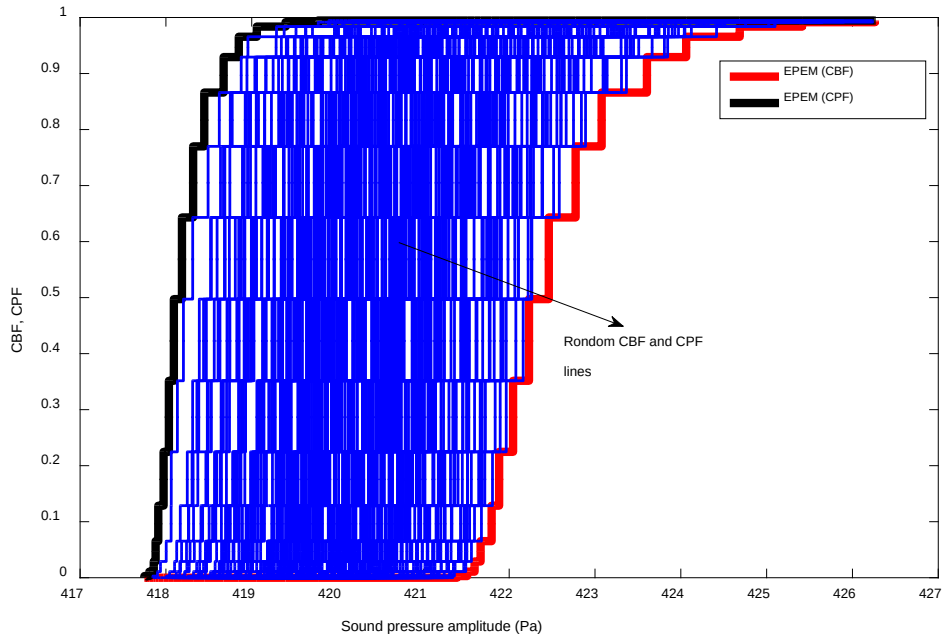

Fig. 11 The CBF and CPF of the sound pressure amplitude at node A (50 Hz)

The 90% interpercentile range of sound pressure amplitude at node A under optimistic and conservative estimation for f = 50-200 Hz is depicted in Fig. 12. It can

be also founded that the lower and upper bounds of the conservative estimation are bigger than that of the optimistic estimation because usually more confronting situations are considered in the conservative estimation than those considered in the optimistic estimation.

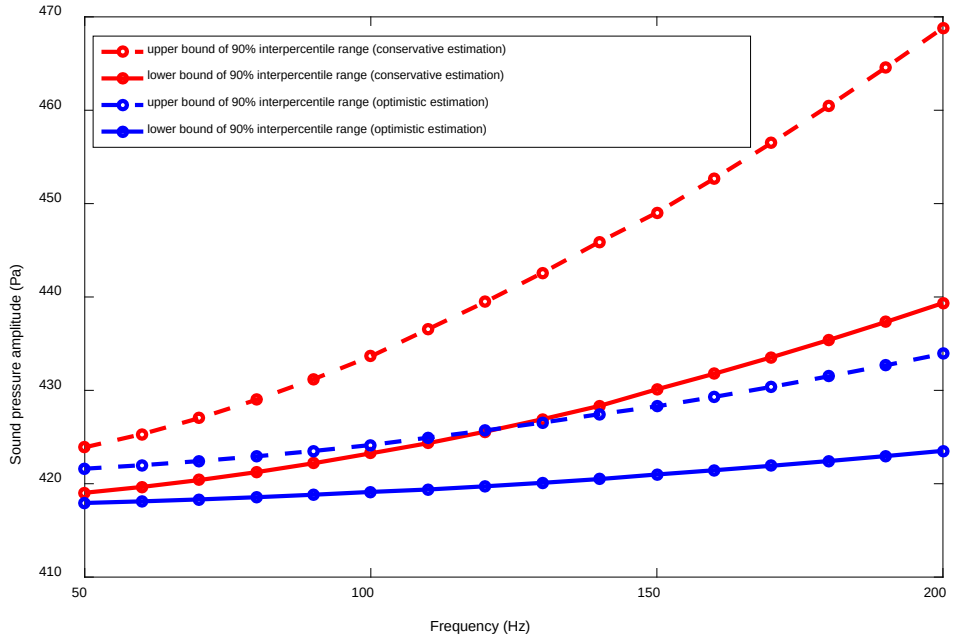

Fig. 12 The 90% interpercentile range of sound pressure amplitude at node A under optimistic and conservative estimation for f = 50-200 Hz

In practical engineering, acoustic behavior is considered when we are conducting the structural design and optimization in order to acquire high level NVH performance. In this process, there is a limit amplitude value at the considered frequency that cannot be exceeded. The limit amplitude value of the frequency response amplitude at the considered frequency is assumed as p_0. $p_{\min}$ and $p_{\max}$ represent the lower and the upper bounds of the calculated frequency response amplitude through the proposed EPEM. Fig. 13 shows the CBF and CPF of the sound pressure amplitude at node A calculated by EPEM when α =0.2. The considered frequency is 200 Hz. When p_0 satisfies $p_0 \geq p_{\max}$, it indicates that the acoustic

performance of the automobile passenger compartment satisfies the design demand perfectly. On the other hand, $p_0 \le p_{\min}$ means a total failure for the design. When p_0 satisfies $p_{\min} \le p_0 \le p_{\max}$, as shown in Fig. 13, the cumulative plausibility value P_0 is larger than the cumulative belief value B_0. This is because P_0 is the cumulative plausibility probability, which is an optimistic estimation, and it is the summation of probability of the events that are totally or partially included in $x \le p_0$. While B_0 is the cumulative belief probability, which is a conservative estimation, and it is the summation of probability of the events that are totally included in $x \le p_0$. In other words, the optimistic and conservative reliability of the structural design considering acoustic behavior can be estimated by comparing the result obtained by the EPEM with the desired demand. Thus, the proposed method for periodical composite structural-acoustic problems with multi-scale mixed aleatory and epistemic uncertainties can play an important role in practical acoustic design and optimization.

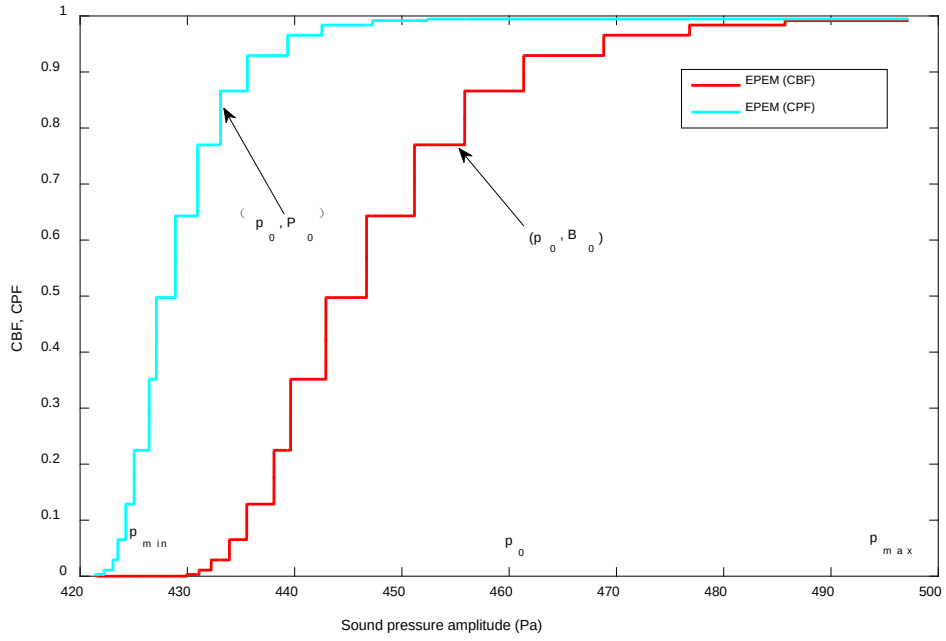

Fig. 13 The CBF and CPF of the sound pressure amplitude at node A and f = 200 Hz

6. Conclusions

Due to the inherent variation of the physical system and environment as well as the incomplete or inaccurate information, the periodical composite structural-acoustic problems are inevitable involved with aleatory and epistemic uncertainties in engineering practice. These uncertainties may lead to significant fluctuation of acoustical behavior of the engineering system. This paper has presented a polynomial expansion approach for the periodical composite structural-acoustic problems with multi-scale mixed aleatory and epistemic uncertainties. The aleatory uncertainties are presented by bounded random variables, whereas the epistemic uncertainties are presented by interval variables and evidence variables. In the periodical composite structural-acoustic system, the macro plate structure is assumed to be composed of a periodic uniform microstructure and the equivalent macro material properties of the microstructure are computed through the homogenization method.

When dealing with the combination of bounded random variables, interval variables and evidence variables in the periodical composite structural-acoustic systems, huge computation is needed to estimate the output probability bounds of the sound pressure. Evidence theory is a powerful tool to deal with the epistemic uncertainties. In addition, the evidence variable can approximate bounded random variable and interval variable under different conditions. Therefore, to reduce the involved enormous computational cost for estimating the output probability bounds of the sound pressure response but without losing accuracy, all of the bounded random variables and interval variables are transformed into evidence variables appropriately.

Then an Evidence-theory-based Polynomial Expansion Method (EPEM) is developed to analysis the periodical composite structural-acoustic system with multi-scale evidence variables. In EPEM, the Gegenbauer series expansion is adopted to approximate the sound pressure response of the periodical composite structural-acoustic system in this paper. It should be noted that there are numerous orthogonal polynomial approximation methods can be applied on the analysis for periodical composite structural-acoustic problem with multi-scale evidence variables. The used Gegenbauer series expansion is just one of these polynomial approximation methods that can approximate the response of the system with enough accuracy. Furthermore, the accuracy of the proposed method is also affected by the selected number of the focal elements when the bounded random variable is transformed into evidence variable. The larger number of focal elements indicates higher accuracy, but means more computational amount. Fortunately, a relatively small number of focal elements can ensure a relatively high accuracy. A numerical example is used to validate the proposed EPEM and two engineering examples are given to demonstrate its efficiency. The results show that the EPEM has a good performance in analysis the periodical composite structural-acoustic system with multi-scale mixed aleatory and epistemic uncertainties. Additionally, the EPEM is a non-intrusive approach and therefore can be extended to other engineering problems with mixed aleatory and epistemic uncertainties easily.

Acknowledgments

The paper is supported by the Key Project of Science and Technology of Changsha (Grant No. KQ1703028) and the Fundamental Research Funds for the Central Universities (531107051148). The author would also like to thank reviewers for their valuable suggestions.

Appendix A. Evidence theory

Evidence theory is also known as the Dempster–Shafer theory. Major concepts of this theory are summarized in this section.

A.1. Fundamental theory of evidence theory

Evidence theory starts on the specification of a frame of discernment (FD), which is a nonempty finite set of mutually exclusive and exhaustive hypotheses $\Theta = \{\theta_1, \theta_2, ...\}$. Under evidence theory, a probability can be assigned for any possible subset of the FD based on the experimentation or expert opinion. This probability is called as Basic Probability Assignment (BPA). The BPA can not only be assigned on a single event but also a set of events, thus it is able to represent the imprecise probability information. The BPA of an event can be denoted by a mapping function $m: 2^{\Theta} \to [0,1]$, where 2^{Θ} represents all possible subsets of Θ. For a given evidential event A, the BPA should satisfy the following three axioms

$$\begin{cases} m(A) \geq 0, \ \forall A \in 2^{\Theta} \\ m(\varnothing) = 0, \\ \sum_{A \in 2^{\Theta}} m(A) = 1 \end{cases} \tag{A.1}$$

where each subset $m(A) \in 2^{\Theta}$ satisfying $m(A) > 0$ is called as the focal element.

Due to the lack of knowledge or information, the evidence theory cannot provide a precise probability for any possible proposition B. Therefore, an interval that consists of the belief and plausibility measures is used to treat the uncertainty of probability of the system response. These two measures can be defined as

$$\mathrm{Bel}(B) = \sum_{A \subseteq B} m(A) \tag{A.2}$$

$$\mathrm{Pl}(B) = \sum_{A \cap B \neq \varnothing} m(A)\,. \tag{A.3}$$

In the above equations, the belief measure Bel(B) is obtained by summing the BPA of proposition which are totally included in B and it indicates the minimum amount of likelihood that could be associated with the event B. Whereas, the plausibility measure Pl(B) is the summation of BPA of propositions which are totally or partially included in B and it indicates the maximum amount of likelihood associated with B. Therefore, Bel and Pl can be viewed as the lower and upper bounds of the probability measure, which bracket the true probability of a proposition. Since no assumptions were made to obtain these measures, Bel and Pl are reasonably consistent with the given partial evidences.

In engineering practices, the cumulative probability of the response can be of guidance for design and optimization of the acoustic system with random variables. Inspired by the cumulative distribution functions (CDF) $p(X \le x)$ in probability theory, the cumulative belief function (CBF) and the cumulative plausibility function (CPF) [37] are introduced and defined as

$$\mathrm{CBF}(x) = \mathrm{Bel}(X \le x)\,, \quad \mathrm{CPF}(x) = \mathrm{Pl}(X \le x) \tag{A.4}$$

where x is an arbitrary value, and X denotes the response of interest such as the sound

pressure.

A.2. Uncertainty qualification of a function using evidence theory

Practical problems always include more than one evidence variable. Consider a general function *G* with *L*-dimensional independent evidence variables.

$$G = G(\mathbf{A}), \quad \mathbf{A} = [A_1, A_2, ..., A_L]. \tag{A.5}$$

Similar to the joint PDF in probability theory, the joint frame of discernment (FD) for evidence variables vector **A** can be defined by using the Cartesian product and denoted by **W**

$$\mathbf{W} = \prod_{i=1}^{L} A_i \,. \tag{A.6}$$

The *k*th focal element of the joint FD can be expressed as

$$\mathbf{W}_k = [a_1, a_2, ..., a_L], a_j \in A_j, j = 1, 2, ..., L, k = 1, 2, ..., n_s \,. \tag{A.7}$$

Where, a_j denotes the focal element of A_j, $\mathbf{W}_k$ denotes the *k*th focal element of the joint FD, n_s is the total number of $\mathbf{W}_k$. Supposing the number of focal elements for the *j*th evidence variable is l_j (j = 1, 2, . . . , L), then the total number of $\mathbf{W}_k$ is $n_s = l_1 \times l_2 \times \cdots \times l_L$. The joint BPAs (Basic Probability Assignments) can be expressed as

$$m(\mathbf{W}_k) = \begin{cases} \prod_{j=1}^{L} m(a_j), & a_j \subseteq A_j \\ 0, & else \end{cases} \tag{A.8}$$

As a function of evidence variables, the output $G(\mathbf{A})$ for each joint focal element $\mathbf{W}_k$ can be represented by an interval with its corresponding BPA. The interval of $G(\mathbf{A})$ over $\mathbf{W}_k$ can be expressed as

$$G_{\mathbf{W}_k}^I = [\underline{G}_{\mathbf{W}_k}, \bar{G}_{\mathbf{W}_k}] = [\min_{\mathbf{A}\in\mathbf{W}_k} G(\mathbf{A}), \max_{\mathbf{A}\in\mathbf{W}_k} G(\mathbf{A})]. \tag{A.9}$$

And the BPA for $G_{\mathbf{W}_k}^I$ is determined by

$$m\left(G_{\mathbf{W}_k}^I\right) = \begin{cases} m(\mathbf{W}_k) \\ 0, \quad else \end{cases} \tag{A.10}$$

Appendix B. Gegenbauer series expansion method

In this section, we briefly summarize the definitions of Gegenbauer expansion. Besides, the weighted least squares method and the Gauss-Gegenbauer integration method is introduced to calculate the coefficients of Gegenbauer expansion.

B.1. Gegenbauer series expansion theory

Using the sums of Gegenbauer polynomials of independent variables to approximate the uncertain analysis process is the basic idea of Gegenbauer series expansion [20]. The *n*-degree Gegenbauer polynomials denoted by $G_n(\xi)$ can be defined by the recurrence relations as follows

$$\begin{cases} G_0^\lambda(\xi) = 1 \\ G_1^\lambda(\xi) = 2\lambda\xi \\ (n+1)G_{n+1}^\lambda(\xi) = 2(n+\lambda)\xi G_n^\lambda(\xi) - (n+2\lambda-1)G_{n-1}^\lambda(\xi), \qquad n \geq 2 \end{cases} \tag{B.1}$$

Where, λ is a polynomial parameter which satisfies $\lambda > 0$.

On $\xi \in [-1, 1]$, the Gegenbauer polynomials are orthogonal in regard to the weight function $\rho^\lambda(\xi)$, and the relations are as follows

$$\int_{-1}^{1} \rho^\lambda(\xi) G_i^\lambda(\xi) G_j^\lambda(\xi) d\xi = \begin{cases} h_i^\lambda, & i = j \\ 0, & i \neq j \end{cases} \tag{B.2}$$

Where h_i^λ and $\rho^\lambda(\xi)$ can be calculated by the following expressions

$$h_i^\lambda = \frac{2^{1-2\lambda}\pi\ \Gamma(i+2\lambda)}{i!(1+\lambda)\Gamma^2(\lambda)} \tag{B.3}$$

$$\rho^{\lambda}(\xi)=\kappa_{\lambda}(1-\xi^{2})^{\lambda-\frac{1}{2}},\ \kappa_{\lambda}=\frac{\Gamma(\lambda+1)}{\Gamma(1/2)\Gamma\left(\lambda+(1/2)\right)}. \tag{B.4}$$

In the above equations, $\Gamma(\bullet)$ stands for the Gamma function. The continuous function $f(\xi)$ defined on $\xi\in[-1,1]$ can be approximated by a combination of Gegenbauer polynomials, which is below order *N*.

$$f(\xi)\approx p_N(\xi)=\sum_{i=0}^{N} f_i G_i^{\lambda}(\xi) \tag{B.5}$$

Where f_i is the ith (i = 0, 1,…, *N*) expansion coefficient, and it can be estimated by using the weighted least squares method and the Gauss-Gegenbauer integration formula, which will be introduced in the following content.

The function discussed above is a single-dimensional function, as for a *L*-dimensional function, it can be expanded by Gegenbauer series as

$$f(\xi)=\sum_{i_1=0}^{N_1}\cdots\sum_{i_L}^{N_L} f_{i_1,\ldots,i_L} G_{i_1,\ldots,i_L}(\xi) \tag{B.6}$$

Similarly, $f_{i_1,\cdots i_L}$ is the expansion coefficient, N_l (l =1, 2,…, *L*) is the retained order of Gegenbauer series corresponding to the *l*th variable ξ_l. And $G_{i_1,\cdots i_L}(\xi)$ is *L*-dimensional Gegenbauer polynomials, which can be expressed as

$$G_{i_1,\cdots i_L}(\xi)=G_{i_1}^{\lambda_1}(\xi_1)\cdots G_{i_L}^{\lambda_L}(\xi_L). \tag{B.7}$$

B.1. Calculation of the expansion coefficients of Gegenbauer series

The weighted residual method can be used to calculate the expansion coefficients of the Gegenbauer series. Galerkin technique is one of the weighted residual methods, which is widely used. However, the transformed equation deduced by Galerkin technique gets a much larger dimension than the degrees of freedom of the original system. The weighted least squares method and the Gauss-Gegenbauer integration

formula can avoid this shortcoming, and then are introduced to calculate the expansion coefficients in this paper.

Firstly, the weighted least squares method is applied to minimize the weighted least squares error R

$$R = \int_{-1}^{1} \rho^{\lambda}(\xi)(e_N)^2 d\xi \tag{B.8}$$

Where, e_N indicate the difference between the Gegenbauer series $p_N(\xi)$ and original function $f(\xi)$, and it can be expressed as

$$e_N = \left| f(\xi) - p_N(\xi) \right| = \left| f(\xi) - \sum_{j=0}^{N} f_j G_j^{\lambda}(\xi) \right|. \tag{B.9}$$

According to the weighted least squares method, the following condition should be satisfied to minimize R

$$\frac{\partial R}{\partial f_i} = 0 \quad , i = 0, 1, 2,\ldots, N. \tag{B.10}$$

By substituting Eqs. (B.5) and (B.6) into Eq. (B.7), one gets

$$\int_{-1}^{1} \rho^{\lambda}(\xi) G_i^{\lambda}(\xi) G_j^{\lambda}(\xi) d\xi = \int_{-1}^{1} \left(\sum_{j=0}^{N} f_j G_j^{\lambda}(\xi) \right) G_i^{\lambda}(\xi) \rho^{\lambda}(\xi) d\xi \, , \; i = 0, 1, 2,\ldots, N. \tag{B.11}$$

Taken that each $G_j^{\lambda}(\xi)$ for $j = 0, 1, 2,\ldots, N$ is orthogonal to $G_i^{\lambda}(\xi)$, we simplify the Eq. (B.11) as

$$f_i = \frac{1}{h_i^{\lambda}} \int_{-1}^{1} \rho^{\lambda}(\xi) f(\xi) G_i^{\lambda}(\xi) d\xi \, , \; i = 0, 1, 2,\ldots, N. \tag{B.12}$$

Then, the coefficient f_i in Eq. (B.12) can be calculated by using the Gauss-Gegenbauer integration formula, which can be expressed as

$$f_i = \frac{1}{h_i^{\lambda}} \int_{-1}^{1} \rho^{\lambda}(\xi) f(\xi) G_i^{\lambda}(\xi) d\xi \approx \frac{1}{h_i^{\lambda}} \sum_{j=1}^{m} f(\hat{\xi}_j^{\lambda}) G_i(\hat{\xi}_j^{\lambda}) A_j^{\lambda} . \tag{B.13}$$

Where, $\hat{\xi}_j^{\lambda}$ (j = 1, 2,…, m) denote the interpolation points, which are the roots of the $G_i^{\lambda}(\xi)$; m is the number of interpolation points, and the weight coefficient A_j^{λ} (j = 1, 2,…, m) can be calculated by using the following expression [46].

$$A_j^{\lambda}=2^{2-2\lambda}\pi\left\{\Gamma(\lambda)\right\}^{-2}\frac{\Gamma(m+2\lambda)}{\Gamma(m+1)}(1-x_j^2)^{-1}\left\{G_m^{\lambda'}(x_j)\right\}^{-2},\ j=1,2,\ldots,m \tag{B.14}$$

where

$$G_m^{\lambda'}=2\lambda G_{m-1}^{\lambda+1}. \tag{B.15}$$

Similarly, the expression of $f_{i_1,\cdots i_L}$ for L-dimension Gegenbauer polynomials can be expressed as

$$\begin{aligned} f_{i_1,\cdots i_L} &= \frac{1}{h_i^{\lambda}\times\cdots\times h_L^{\lambda_L}}\int_{-1}^{1}\cdots\int_{-1}^{1}\rho_{i_1,\ldots,i_L}(\xi)f(\xi)G_{i_1,\ldots,i_L}(\xi)d\xi_1\cdots d\xi_L \\ &\approx \frac{1}{h_i^{\lambda}\times\cdots\times h_L^{\lambda_L}}\sum_{j_1=1}^{m_1}\cdots\sum_{j_L}^{m_L}f(\hat{\xi}_{j_1},\ldots,\hat{\xi}_{j_L})G_{i_1,\ldots,i_L}(\hat{\xi}_{j_1},\ldots,\hat{\xi}_{j_L})A_{j_1,\ldots,j_L} \end{aligned} \tag{B.16}$$

where $\hat{\xi}_{j_1},\ldots,\hat{\xi}_{j_L}$ are the interpolation points, the weight $A_{j_1,\ldots,j_L}$ can be expressed as

$$A_{j_1,\ldots,j_L}=A_{j_1}^{\lambda_1}\times A_{j_2}^{\lambda_2}\times\cdots\times A_{j_L}^{\lambda_L}. \tag{B.17}$$

From the above analysis, we can conclude that the Gegenbauer series expansion for the original functions can be derived by several iterative computations in which we need to calculate the function value at the interpolation points (see in Eq. (B.16)). Generally, with the number of integration points increasing to $m_i = N_i + 1$, the integration method can achieve high accuracy. In this paper, the integration points are set as $m_i = N_i + 1$. According to Eq. (B.16), the total number of integration points can be determined by

$$N_{tot}=(N_1+1)\times(N_2+1)\times\cdots\times(N_L+1). \tag{B.18}$$

References

[1] He, Z. C., Liu, G. R., Zhong, Z. H., Zhang, G. Y., & Cheng, A. G. (2010). Coupled analysis of 3d structural–acoustic problems using the edge-based smoothed finite element method/finite element method. Finite Elements in Analysis & Design, 46(12), 1114-1121.

[2] Xia, B., Yu, D., & Liu, J. (2013). Hybrid uncertain analysis for structural–acoustic problem with random and interval parameters. Journal of Sound & Vibration, 332(11), 2701-2720.

[3] Chen, N., Yu, D., & Xia, B. (2014). Hybrid uncertain analysis for the prediction of exterior acoustic field with interval and random parameters. Computers & Structures, 141, 9-18.

[4] Xu, M., Qiu, Z., & Wang, X. (2014). Uncertainty propagation in sea for structural–acoustic coupled systems with non-deterministic parameters. Journal of Sound & Vibration, 333(17), 3949-3965.

[5] Yin, S., Yu, D., Yin, H., & Xia, B. (2016). Interval and random analysis for structure–acoustic systems with large uncertain-but-bounded parameters. Computer Methods in Applied Mechanics & Engineering,305, 910-935.

[6] Xia, B., & Yu, D. (2015). Optimization based on reliability and confidence interval design for the structural-acoustic system with interval probabilistic variables. Journal of Sound & Vibration, 336, 1-15.

[7] Chen, N., Yu, D., Xia, B., Liu, J., & Ma, Z. (2017). Homogenization-based interval analysis for structural-acoustic problem involving periodical composites and multi-scale uncertain-but-bounded parameters. Journal of the Acoustical Society of America, 141(4), 2768.

[8] Hoffman, F. O., & Hammonds, J. S. (1994). Propagation of uncertainty in risk assessments: the need to distinguish between uncertainty due to lack of knowledge and uncertainty due to variability. Risk Analysis, 14(5), 707–712.

[9] Spanos, P. D., & Kontsos, A. (2008). A multiscale monte carlo finite element method for determining mechanical properties of polymer nanocomposites. Probabilistic Engineering Mechanics, 23(4), 456-470.

[10] Hurtado, J. E., & Barbat, A. H. (1998). Monte carlo techniques in computational stochastic mechanics. Archives of Computational Methods in Engineering, 5(1), 3.

[11] Doltsinis, I., & Kang, Z. (2006). Perturbation-based stochastic fe analysis and robust design of inelastic deformation processes. Computer Methods in Applied Mechanics & Engineering, 195(19–22), 2231-2251.

[12] Kamiński, M. M. (2010). A generalized stochastic perturbation technique for plasticity problems. Computational Mechanics, 45(4), 349.

[13] Rong, B., Rui, X., & Tao, L. (2012). Perturbation finite element transfer matrix method for random eigenvalue problems of uncertain structures. JOURNAL OF APPLIED MECHANICS-TRANSACTIONS OF THE ASME, 79(2), 1005.

[14] B. S. Lazarov, Schevenels, M., & O. Sigmund. (2012). Topology optimization

with geometric uncertainties by perturbation techniques. International Journal for Numerical Methods in Engineering, 90(11), 1321–1336.

[15] Ghanem, R. G., & Spanos, P. D. (1992). Stochastic Finite Elements: A Spectral Approach. Springer-Verlag.

[16] Wiener, N. (1938). The homogeneous chaos. American Journal of Mathematics, 60(4), 897-936.

[17] Nouy, A. (2009). Recent developments in spectral stochastic methods for the numerical solution of stochastic partial differential equations. Archives of Computational Methods in Engineering, 16(3), 251-285.

[18] Xiu, D., & Karniadakis, G. E. (2002). The Wiener--Askey Polynomial Chaos for Stochastic Differential Equations. SIAM J. SCI. COMPUT(Vol.24, pp.619--644).

[19] M.D. Shields, & Deodatis, G. (2013). A simple and efficient methodology to approximate a general non-gaussian stationary stochastic vector process by a translation process with applications in wind velocity simulation. Probabilistic Engineering Mechanics, 31(31), 19-29.

[20] Wu, C. L., Ma, X. P., & Fang, T. (2006). A complementary note on gegenbauer polynomial approximation for random response problem of stochastic structure. Probabilistic Engineering Mechanics, 21(4), 410-419.

[21] Ben-Haim, Yakov, Elishakoff, & Isaac. (1990). Convex models of uncertainty in applied mechanics. Elsevier.

[22] Elishakoff, I., Elisseeff, P., & Glegg, S. A. L. (2012). Nonprobabilistic,

convex-theoretic modeling of scatter in material properties. Aiaa Journal,32(4), 843-849.

[23] Mourelatos, Z. P., & Zhou, J. (2005). Reliability estimation and design with insufficient data based on possibility theory. Aiaa Journal, 43(8), 1696-1705.

[24] Mcwilliam, S. (2001). Anti-optimisation of uncertain structures using interval analysis. Computers & Structures, 79(4), 421-430.

[25] JamesInglis. (1976). A mathematical theory of evidence. Technometrics,20(1), 106-106.

[26] Chen, N., Yu, D., & Xia, B. (2015). Evidence-theory-based analysis for the prediction of exterior acoustic field with epistemic uncertainties. Engineering Analysis with Boundary Elements, 50, 402-411.

[27] Guan, J. W., & Bell, D. A. (1991). Evidence Theory and Its Applications. Elsevier Science Inc.

[28] Rao, S. S., & Berke, L. (1997). Analysis of uncertain structural systems using interval analysis. Aiaa Journal, 35(4), 727-735.

[29] Sofi, A., & Romeo, E. (2016). A novel interval finite element method based on the improved interval analysis. Computer Methods in Applied Mechanics & Engineering, 311, 671-697.

[30] Sofi, A., Muscolino, G., & Elishakoff, I. (2015). Natural frequencies of structures with interval parameters. Journal of Sound & Vibration, 347, 79-95.

[31] Qiu, Z., & Lv, Z. (2017). The vertex solution theorem and its coupled framework

for static analysis of structures with interval parameters. International Journal for Numerical Methods in Engineering, 112.

[32] Qiu, Z., Chen, S., & Elishakoff, I. (1996). Bounds of eigenvalues for structures with an interval description of uncertain-but-non-random parameters. Chaos Solitons & Fractals, 7(3), 425-434.

[33] Qiu, Z., & Elishakoff, I. (1998). Antioptimization of structures with large uncertain-but-non-random parameters via interval analysis. Computer Methods in Applied Mechanics & Engineering, 152(3), 361-372.

[34] Impollonia, N., & Muscolino, G. (2011). Interval analysis of structures with uncertain-but-bounded axial stiffness. Computer Methods in Applied Mechanics & Engineering, 200(21–22), 1945-1962.

[35] Degrauwe, D., Lombaert, G., & De Roeck, G. (2010). Improving interval analysis in finite element calculations by means of affine arithmetic. Computers & Structures, 88(3–4), 247-254.

[36] Wu, J., Zhang, Y., Chen, L., & Luo, Z. (2013). A chebyshev interval method for nonlinear dynamic systems under uncertainty. Applied Mathematical Modelling, 37(6), 4578-4591.

[37] Yin, S., Yu, D., Yin, H., & Xia, B. (2017). A new evidence-theory-based method for response analysis of acoustic system with epistemic uncertainty by using jacobi expansion. Computer Methods in Applied Mechanics & Engineering, 322.

[38] Bae, H. R., Grandhi, R. V., & Canfield, R. A. (2004). An approximation approach

for uncertainty quantification using evidence theory. Reliability Engineering & System Safety, 86(3), 215-225.

[39] Bae, H. R., Grandhi, R. V., & Canfield, R. A. (2004). Epistemic uncertainty quantification techniques including evidence theory for large-scale structures. Computers & Structures, 82(13), 1101-1112.

[40] Gao, W., Song, C., & Tin-Loi, F. (2010). Probabilistic interval analysis for structures with uncertainty. Structural Safety, 32(3), 191-199.

[41] Bendsøe, M. P., & Kikuchi, N. (1988). Generating optimal topologies in structural design using a homogenization method. Computer Methods in Applied Mechanics & Engineering, 71(2), 197-224.

[42] M. P. Bendsøe, & O. Sigmund. (2004). Topology optimization. theory, methods, and applications. 2nd ed. corrected printing.

[43] Xia, B., & Yu, D. (2014). An interval random perturbation method for structural - acoustic system with hybrid uncertain parameters. International Journal for Numerical Methods in Engineering, 97(3), 181-206.

[44] Stefanou, G. (2009). The stochastic finite element method: past, present and future. Computer Methods in Applied Mechanics & Engineering,198(9–12), 1031-1051.

[45] Shah, H., Hosder, S., & Winter, T. (2015). Quantification of margins and mixed uncertainties using evidence theory and stochastic expansions. Reliability Engineering & System Safety, 138, 59-72.

[46] Szegő, G. (1979). Orthogonal Polynomials. Orthogonal polynomials. American Mathematical Society.